ELSEVIER

Nuclear Instruments and Methods in Physics Research A 357 (1995) 71–77

NUCLEAR INSTRUMENTS & METHODS IN PHYSICS RESEARCH Section A

Development of fiber-to-fiber connectors for scintillating tile/fiber calorimeters

S. Aota [a], R.C. Bossert [b], S. Fukuda [c], K. Hara [a,*], H. Kawamoto [a], S. Kim [a], K. Kondo [a], M. Mishina [d], H. Nakada [a], H. Sato [c], Y. Seiya [a], K. Takikawa [a]

[a] *Institute of Physics, University of Tsukuba, Tsukuba-shi, Ibaraki-ken 305, Japan*
[b] *Fermi National Accelerator Laboratory, Batavia, IL 60510, USA*
[c] *R & D Division, DDK Co. Ltd., 14 Matsuyama, Mouka-shi, Ibaraki-ken 321-43, Japan*
[d] *National Laboratory for High Energy Physics, KEK, Tsukuba-shi, Ibaraki-ken 305, Japan*

Received 2 September 1994

Abstract

We have developed fiber-to-fiber connectors for plastic fibers of 0.83, 0.90, and 1.00 mm in diameter. Such a connector is essential for detectors that use a large number of optical fibers, scintillating or clear. Typical applicators are unscintillating tile/fiber calorimetry and scintillating fiber tracking. We describe the design and performance of two types of small 10-fiber connectors which were developed for the CDF endplug tile/fiber calorimeter. The connectors showed a light transmission of 85–90% with a uniformity of 2.5–3.1%, and a reproducibility of 1%. Use of optical matching material at the joints could further improve the transmission and uniformity but showed instability after heat cycles.

1. Introduction

Multi-channel fiber-to-fiber connectors are needed to handle a large number of fibers from detectors such as scintillating tile/fiber calorimeters including shower maximum detectors, and scintillating fiber trackers, where the number of fibers may be of the order of hundreds of thousands. Connectors simplify fiber routing and thus assembly, which allows handling fibers without causing damage and provides correct connection of the channels. It also modularizes the system, which is essential for debugging the system, testing, and calibrating detector components before assembling them into the final complete detector.

The CDF endplug upgrade project [1] is an absorber-scintillator sandwich calorimeter and "tile/fiber" technique is used to make a finely segmented projective tower geometry in the pseudorapidity range of 1.1 and 3.5. The electromagnetic calorimeter (EM) is composed of 23 layers of 4.5 mm lead clad with 0.5 mm stainless steel sheet on both sides interleaved with 4 mm thick polystyrene scintillator tile layers. The hadronic calorimeter (HAD) behind is a 22 layer sandwich of 50.8 mm steel plates with 6 mm scintillator. There will be a scintillator strip layer inserted in the 5th layer, the "shower max detector", that measures the lateral profile of the shower in two dimensions by two sets of 5 mm wide scintillator strips crossing at 45° with respect to each other.

The lateral segmentation of the EM calorimeter is shown in Fig. 1. In the EM section, 20 tiles in 15° in azimuthal angle are housed in a package called a "pizza pan" with thin top and bottom plastic sheets. Each of the 0.83 mm waveshifting fibers embedded in a groove along the perimeter of each of the tiles is spliced [2] to a clear fiber by a thermal fusion technique at a point when the waveshifting fiber exits the tile. Then the clear fibers from all 20 tiles are gathered to two connectors called type A which are mounted near to the outer circular edge of the pizza pan. From these connectors to the rear end of the calorimeter where phototubes are mounted, light from the tiles is guided by 10-fiber cables routed through a 2.5 cm gap between the endplug structure and the central structure of CDF. Each cable is made of ten 0.9 mm clear fibers covered with a dark Tedler sheath and have a type A connector on the end to be mated with the connector on the pizza pans and a type B connector on the other end which mates to the same type of connector on a "decoding box" in front of the phototubes. The decoding box rearranges the fiber order in the incoming cables from each pizza pan to tower-by-tower order for the phototubes using 1.0 mm clear fibers. The length of the cables is about 3 m each.

* Corresponding author.

SSDI 0168-9002(94)01523-6

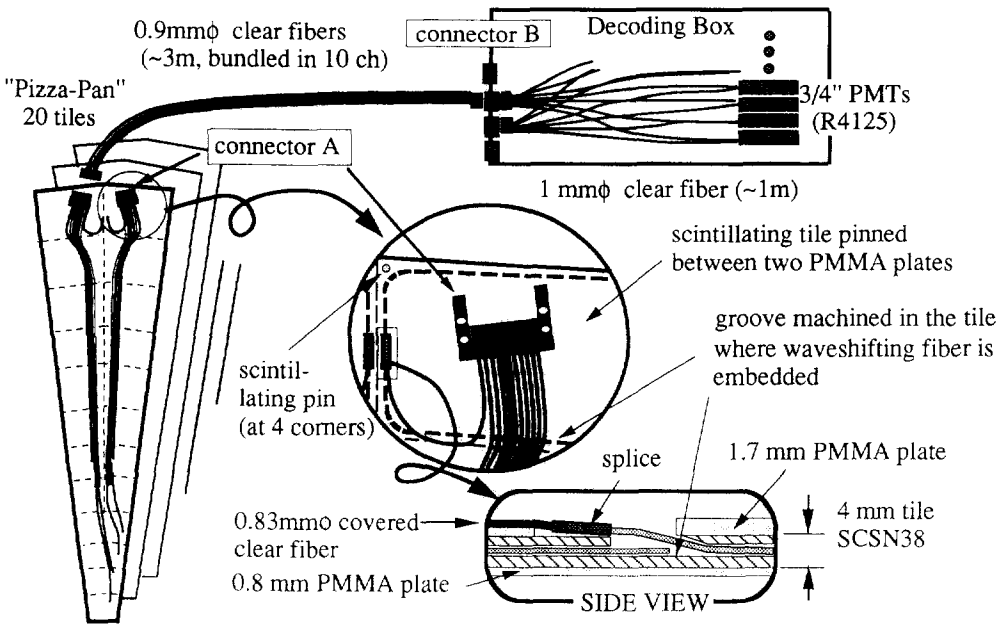

Fig. 1. Optical system in the CDF endplug upgrade calorimeter. The signals from 20 scintillating tiles grouped as a "pizza pan" are readout through optical fiber cables which are inter-connected by two connectors A and B.

The requirement for the HAD section is quite similar except that the tiles are packaged into units of 30° in azimuth and four 10-fiber connectors are mounted on each of the units. These connectors are type B with fiber diameter of 0.83. The cables for the HAD are also made with 0.9 mm clear fibers with type B connector on both sides.

We have designed these two types of connectors [3] and produced 2208 pairs each for the EM section. For the HAD section, 2112 pairs of type B for 0.83–0.9 mm connection and the same number of type B for 0.9–1.0 mm connection are used. The shower max detector is also based on a fiber readout technique, and the readout connectors and cables are similar to those for the EM section.

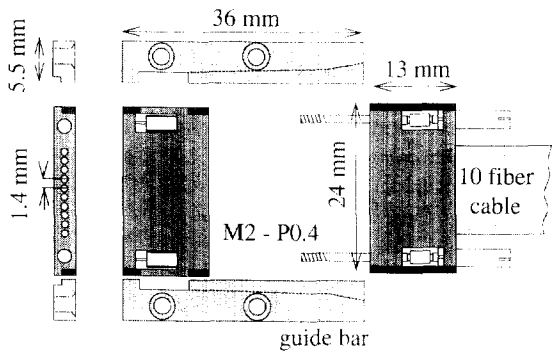

Fig. 2. Schematic drawing of the type A connector. The cable assemblies are mated by two screws, and positioned by the guide bars which are screwed to the pizza pan.

In the following sections, we describe the design of the connector and performance tests. The tests include initial light transmission and uniformity, light transmission reproducibility after repeating disconnection and re-connection cycles, and optical and mechanical stability measured under heat cycles. In the CDF calorimeter, we use Kuraray multiclad fibers [4], since they yield larger light output and allow more uniform fiber splices than single-clad fibers. The emission light angle distribution was measured to evaluate the effect of the connector on the light transmission in multiclad and single-clad fibers.

2. Design

2.1. Structure

Fig. 2 shows the structure of the 10-fiber connector, type A. The connector is 36 mm long, 34 mm wide, and 3.2 mm thick. The fiber-to-fiber spacing is 1.4 mm to match that of the fiber cable. The connector is mounted on the surface of the pizza pan whereas the gaps between the lead absorber plates are determined by the thickness of the pizza pan without the connector. Therefore the thickness was kept as small as possible so that the indent in the lead absorber plate to accommodate the connector is minimal. The indent was made by cutting out the part of the lead plate around the connector and filling this cutout with a tungsten panel. The physical thickness of the tungsten panel is 1.6 mm which, with 0.5 mm stainless steel

cladding on one side, is equivalent to the original lead plate in terms of radiation length.

The mating two parts of the connector pair were aligned by two screws at both edges of the connector whose slightly thicker stems act as dowel pins. The connector part which is mounted on the pizza pan is held in place by a pair of brackets screwed down to the surface plate of the pizza pan. The brackets are extended towards the mating parts as a guide so that the mating part can be easily aligned by slipping into the brackets.

The fibers are inserted into the holes of the connector body and epoxied. The mating end is then cut and polished by a flying diamond tool or cut by a regular flying tool and then polished by a polishing machine with abrasive.

We made a study of an alternative method of holding the fibers in U-shaped grooves. However it turned out that the strength of the fiber-connector fit is too sensitive to the dimensional tolerance of the U-grooves and the fiber diameter tolerances. The achievable tensile strength was about 0.63 kg on average but it varied down to 0.3 kg in the worst case. Since our aim was to achieve 1 kg, we have abandoned this method and chosen the epoxying method with which we have not encountered any intrinsic problems.

Another type of connector, type B, is shown in Fig. 3. Type B connectors were developed to connect the other end of the fiber cables to the "decoding box". Type B connectors are also used for the pizza pans for the hadronic section which has enough gap space in the steel absorber structure to accommodate the connector.

The connector is 40 mm long, 27 mm wide and 5 mm thick in overall dimensions. The connector is composed of three parts. The ferrule holds the fiber by epoxying. Then a flange, the second part, is fixed over the ferrule with a latch. The flange has a pair of latches on the sides which hook into a pair of holes on the side wall of the guide, the third part, when the ferrule-flange assembly is pushed in. There is a spring between the ferrule and the flange to push the ferrule against the mating partner within the guide. There are three 0.020 mm high ridges along the direction of the ferrule insertion on the inner wall of the guide which keep the tolerance of the guide tight enough without much friction when the ferrules are inserted.

While the spacing of the holes for fibers are kept the same, 1.4 mm, as in the type A connector, the hole diameters are varied corresponding to three different fiber diameters, 0.83 mm for the connector on the HAD segment pizza pans, 0.9 mm for fiber cables both for EM and HAD segments, and 1 mm for the decoding box. The fiber diameter tolerance was specified to be within $\pm 2\%$ of the nominal diameter and has been kept well within the specified tolerance. Therefore, the hole diameters are specified to be 0.03 mm larger than the nominal fiber diameters to account for the fiber diameter tolerances and also the molding tolerance, 5 μm typically.

In order to quantify the requirements to the precision of the connector dimensions, we measured the light transmission variation as a function of misalignment of the fiber axes, of the gap between the fiber ends, and of the angle of the two fibers. We used a pair of Kuraray multiclad fibers with the movement of the fibers precisely controlled with a micro-stage. While injecting LED lights from one end, we measured the light yield emerging from the other end. The data are summarized in Fig. 4. The results for the axis misalignment are compared between 0.83–0.83 mm ϕ and 0.83–1.00 mm ϕ cases. These two measurements were done with keeping a gap of 0.01 mm.

The loss of overlapping area between two fibers of the same diameter due to misalignment can be calculated by the following formula:

$$\frac{A_{\text{loss}}}{A} = 1 - \frac{2\arccos(d/2r)}{\pi} + \frac{d}{\pi r}\sqrt{1-\left(\frac{d}{2r}\right)^2} \sim \frac{2d}{\pi r}.$$

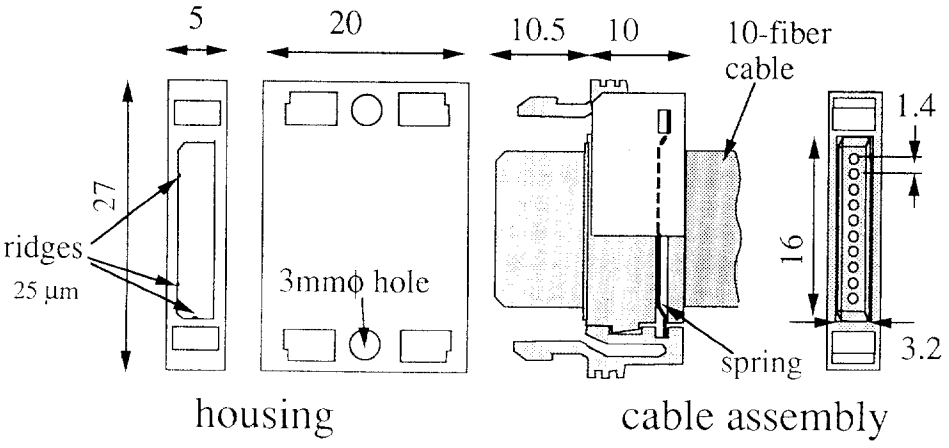

Fig. 3. Schematic drawing of the type B connector. The cable assembly is inserted in the housing and the internal spring keeps the cable assembly from being disconnected.

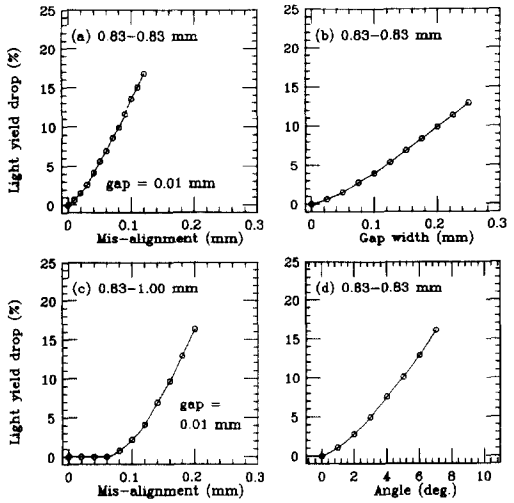

Fig. 4. Effect of geometrical arrangements on the transmission loss. The transmission loss as a function (a) of the axis misalignment for the connection between 0.83 and 0.83 mm ϕ fibers, (b) of the gap between the fibers, (c) of the axis misalignment for the connection from 0.83 to 1.00 mm ϕ fibers, and (d) of the angle of the fibers. The fibers for (b) and (d) are 0.83 mm in diameter.

As noted here, the effect of the misalignment expressed as the fraction of the original light A_{loss}/A is close to the displacement between the fiber axes d measured in the unit of the radius of the fiber r when the displacement is not large. The measured results in Fig. 4a for 0.83–0.83 mm connection is well reproduced by the above calculation. The maximum angle of the light within the multiclad fiber is calculated as follows:

$$\theta_{\max} = \arccos\left(\frac{1.42}{1.59}\right) = 26.7^{\circ},$$

where 1.42 and 1.59 are the refractive indices of the outer cladding and the core, respectively. However, once the light exits the fiber into air, the maximum exit angle is 45.7°. Therefore, any gap between the connected fibers will result in an increase of the diameter of the light flux, as shown in Fig. 4b.

The expected performance of the connector is a uniformity of 2 to 3%, and reproducibility of about 1% for the case of 0.83 to 0.83 mm fiber connection. Oversizing the holes for the fibers by 30 μm introduces an axial misalignment of up to 30 μm for a nominal diameter fiber, which in turn introduces a transmission loss of 2.5% (Fig. 4a). As expected for the connection of 0.83 to 1.00 mm fiber, the misalignment is much more forgiving. Misalignment of up to ~ 80 μm does not induce any transmission loss (Fig. 4c). This result justifies our design of stepping up the fiber diameter at every junction.

For either of the two types of the connectors, the mating ferrules are pressed against each other and the gap, if any, is only due to local deviation from a perfectly flat surface. The above measurement in Fig. 4b indicates that the gap between the two connectors be controlled to smaller than 30 μm to keep the variation smaller than 1%. The relative angle between the mating fibers (Fig. 4d) has to be controlled to be smaller than 1°, or the gap created by the angle at one edge of 10 mm thick ferrule be smaller than 0.17 mm.

2.2. Selection of materials

In designing the connector, we have to choose the materials for the connector body, epoxy, and the optical matching material that reduces the Fresnel reflection.

The connector plastic is liquid-crystal-polymer with 30% glass fiber added, which is selected for superior thermal property (deformation temperature of ~ 200°C) and small shrinkage at molding. The same material combination has been used by DDK for integrated connectors in which good mechanical stability is required. Glass fiber filling was necessitated to achieve the required dimensional tolerances. However, it creates some problems with fiber end preparation. It wears cutting tool bits of either steel or diamond, and glass fiber is often dragged by the bit and scratches the surface of the fiber. Also, it takes much longer to polish these connectors with an abrasive. The condition of the fiber finish needed to be carefully monitored and the diamond bit needed to be replaced periodically. Therefore, glass fiber filled material is not ideal and it is the subject of further study.

Concerning the epoxy, we have tested five types of epoxy, Epotek 353ND and 715, and Cemedine EP-007, EP-330 and EP-331. Among these epoxy, 353ND showed the best adhesion for fluorinated MMA, the outer clad of Kuraray's multiclad fiber, and EP-330 and 715 showed moderate adhesion. We measured the transmission under heat cycles, and observed little temperature dependence with these epoxies. Since EP-330 has been used by DDK for plastic fibers and it can be cured at room temperature, we selected EP-330 for our operation.

There is an intrinsic loss of transmission of ~ 10% due to the inevitable Fresnel reflection if there is an air gap between the mating connectors. We have investigated various index matching materials such as grease and a silicone rubber sheet, both of which showed that the transmission changes after heat cycles. Fig. 5 shows the typical light transmission variations under heat cycles for a type B connector. The temperature was changed from 0°C to 50°C according to the pattern shown in the figure. The light output dropped by ~ 6% at lower temperatures if matching grease, Toray-Dow Corning SC-107, was used, whereas the light output was stable within 0.5% if no matching grease was used. The small light output change for the case with no matching grease can be attributed to the variation of the gap due to different expansions between the fiber and the connector material. The significant change for the case in which grease was used can be explained by

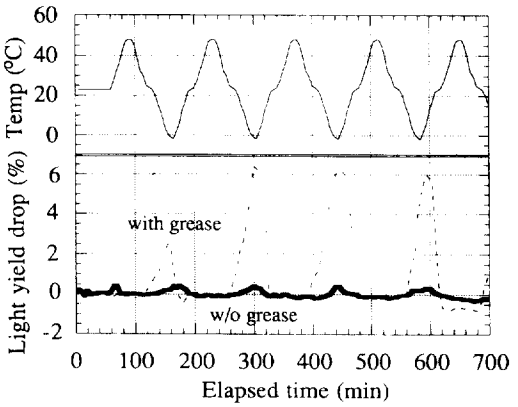

Fig. 5. Heat-cycle test of the type B connector. Light yield variation is plotted for the two cases: optical matching grease was used (dashed curve) and was not used (solid curve). The upper half shows the temperature patten.

the fact that the grease is not viscous enough at lower temperatures and we saw some Fresnel reflection showing up. A similar level of instability was observed for the case where silicon rubber was used as the index matching material. Since the most important feature of the connector is in its reproducibility as opposed to its absolute light yield, we decided to leave the junction with an air gap.

3. Performance

3.1. Light transmission

We measured the light transmission across the connector in the following way. Kuraray multiclad clear fibers of 1 m length were used. Then both ends were furnished with commercially available connectors, DDK 905D. The initial light yield was determined by injecting LED light from one end and measuring, with a photodiode, the light output emerging from the other end. The same fiber was cut at midpoint and furnished with the connector pair under test, and the light yield was measured similarly. The light transmission is defined as the ratio of the two. By definition, the transmission in this case is for the connection of fibers with the same diameter.

Table 1 summarizes the light transmission measurements for the connectors A and B. The transmission was measured for both 0.83 mm ϕ and 0.90 mm ϕ fibers. For the type A connector, the transmission with optical grease was measured for comparison. The average light transmission ranges from 84.9% to 90.3% without using matching grease. Use of matching grease increases the transmission by 3–6% for the type A connector. Slightly better results with 0.90 mm ϕ fibers than with 0.83 mm ϕ can be understood qualitatively from the tolerance in the connector alignment. We surveyed the dimensions of the connectors and housings of the type B connector, and found that the dimensions such as the hole diameters, pitches, connector thickness and width, and housing height vary by 5 to 10 μm. There is a clearance in the hole of 30 μm, in addition, as described before. These finite misalignments degrade the transmission more for the thinner fiber.

The rms transmission nonuniformity ranges from 2.5% to 3.1% without grease and is $\sim$ 1.5% with grease. The transmissions for the type A connector with 0.9 mm ϕ fibers, which showed the largest nonuniformity, 3.1%, are plotted in Fig. 6 as a function of the fiber number 1–10. The nonuniformity between different connectors seems to be larger than that between different fibers within a single connector. This difference can be attributed to the difference in the Fresnel reflection condition. Actually, the transmission of $\sim$ 95% is too high if Fresnel reflection exists. If the fiber ends are flat and pushed closely to each other, the Fresnel reflection is reduced by a partial contact, which seems to be the case for the type A connector where the cable assemblies are screwed together closely. This explains why the type A connector showed better transmission on average and worse nonuniformity than the type B connector.

In the CDF tile/fiber calorimeter, the variation of absolute light transmission of individual light path from a scintillator to the phototube is added in quadrature to the intrinsic tile response variation in a tower which is required to be better than 10%. Therefore, the measured rms variation of $\sim$ 3% is acceptable.

Table 1
Summary of light transmission measurements for connectors A and B, where the number of samples measured, average and rms variation of the transmission, maximum and minimum transmissions are listed. The results were obtained for two fiber diameters, 0.83 and 0.90 mm ϕ. For the type A connector, the data with optical matching grease are shown for comparison

Connector	Fiber diameter [mm ϕ]	#Samples	Average [%]	rms [%]	Maximum [%]	Minimum [%]	Matching
A	0.83	30	86.4	2.9	91.2	79.4	air
A	0.90	30	90.3	3.1	95.3	84.5	air
A	0.83	30	92.3	1.8	95.5	89.3	grease
A	0.90	30	93.6	1.4	95.9	90.2	grease
B	0.83	60	84.9	2.6	88.5	80.2	air
B	0.90	60	86.1	2.5	90.2	80.9	air

3.2. Reproducibility of the light transmission

The reproducibility of the light transmission is one of the most important issues in the development of the connector. In order to achieve good transmission reproducibility, good position reproducibility in terms of, as studied in Fig. 4, gap distance, fiber axis alignment, and fiber angle are necessary as well as good durability of the connector body itself.

The type A connector uses two screws with dowel pin function that determine the position reproducibility. We measured the reproducibility of the type A connector when 0.83 and 0.90 mm ϕ fibers are mated. For a sample of 100 channels (10 connectors), we obtained an rms spread of 0.9% in the light yield variation. The maximum deviation was 1.8%. In this measurement, the screws were tightened at a fixed torque of 1 kg cm. The reproducibility of the type B connector is improved substantially by adding the ridges mentioned before. With the ridges added, the connector clearance in the housing was reduced to 3–28 μm in width and 10–30 μm in height. We measured the reproducibility of the type B connector for the cases where 0.83–0.83 mm ϕ fibers are mated and 0.90–1.00 mm ϕ are mated. For the 0.83–0.83 mm ϕ connection, a total of 450 (45 connectors) reproducibility measurements resulted in an rms variation of 1.1%. For the 0.90–1.00 mm ϕ connections, we measured an rms reproducibility of 1.0% for 100 channels (10 connectors).

Fig. 7 shows the light yield variation of a single sample after multiple reconnection and dis-connection cycles were made up to 50 times. The actual light yield measurements were made every time in 1st through 10th cycles, and at the 15th, 20th, 30th, 40th and 50th cycles. The maximum and minimum light yields among 10 fibers are plotted in the figure. The results are consistent with 1% reproducibility. The connector is proven to be durable up to the 50 re-connections we examined.

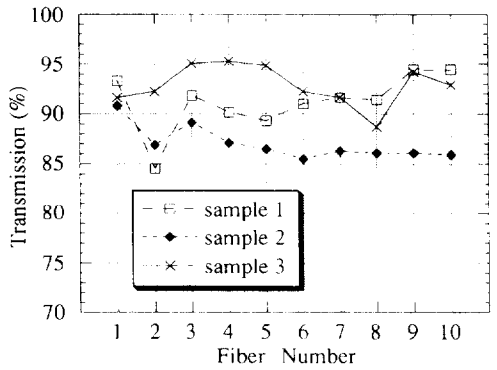

Fig. 6. Transmission measured for three samples of type A connector is shown as a function of the fiber number. The fiber diameter is 0.9 mm and no optical matching grease was used.

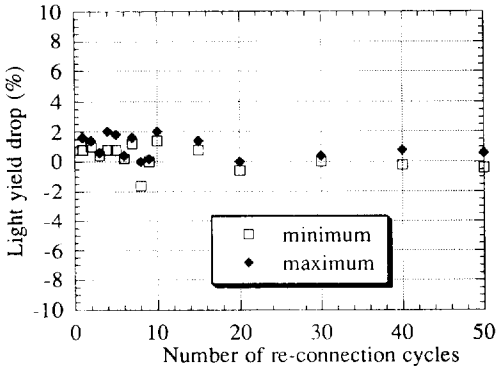

Fig. 7. Durability of the type B connector. Light yield change after multiple disconncetion and re-connection cycles is plotted. After the 10th cycle, the light yield measurements were actually done at those specific times shown in the figure. The maximum and minimum light yield out of the 10 fibers are shown.

3.3. Other tests

In the stage of designing the connector, we performed various other tests. The cross talk, the light yield when the light was injected into the adjacent fiber, was measured to be smaller than 0.1% and was consistent with the background in the measurement system. We investigated the light yield variation after keeping the connector assemblies at $-40°$, which is foreseen when we ship them by airway. The light transmission was stable to within 1–2%. We studied the effect of fiber bending on the light transmission. In this study, the fiber and connector system was bent by $\frac{1}{4}$ turn at a radius of 30 mm, and we measured the light yield with changing the location of the connector in the curvature. The light yield was stable within 1%, independent of where the connector was located.

3.4. Effect of the connector on the light transmission

Kuraray multiclad fibers are used for both the waveshifting and clear fibers. In comparison to single-clad fibers, the larger numerical aperture afforded by the multiclad fibers allows transmission of a larger fraction of the light. The capturing efficiency or the solid angle of the light reflected by the total reflection at the boundary of the inner surface of the outer cladding can be calculated as

$$\Delta\Omega = \tfrac{1}{2}(1 - n_{\text{clad}}/n_{\text{core}}).$$

The refractive indices for the multiclad and the single-clad fibers are $n_{\text{clad}} = 1.42$ and 1.49, respectively, and the $n_{\text{core}} = 1.59$. Therefore $\Delta\Omega = 5.35\%$ and 3.14%, respectively.

Another advantage of the multiclad fiber is its mechanical durability which affects the light transmission in two ways. Firstly, in case of multiclad fiber, the inner cladding is mechanically well protected by the outer cladding, and is transmitting 60% of the light. Secondly, the outer

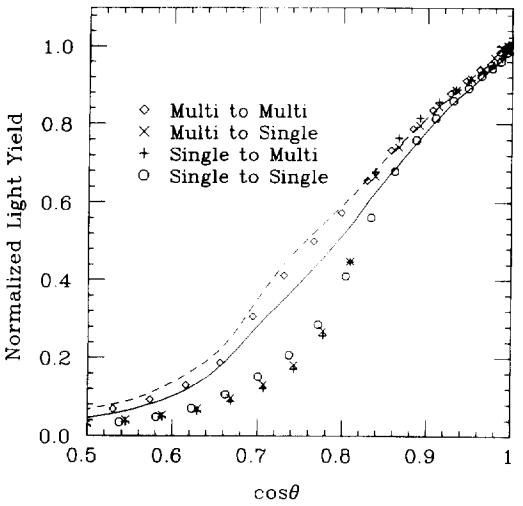

Fig. 8. Emission angle distributions. The data points show the connection of Y11 waveshifting and clear fibers with all four combinations of multiclad and single-clad fibers. The curves show the distributions for single single-clad (solid) and multiclad (dashed) Y11 fibers.

cladding material, fluorinated MMA, is softer and more flexible than the inner cladding material, PMMA, which is rather brittle especially in the form of cladding which is only 30 μm thick. Therefore, the single-clad fiber is more susceptible to scratches and cracks, which directly effect the transmission, because the PMMA is exposed as the only cladding.

The effect of the connector on the light transportation mechanism in the fiber can be evaluated by measuring the angular distribution of light emerging from the fiber end. We measured the emission angle distribution using a computer controlled turning stage. The fiber end of the sample was fixed at the pivot. A phototube which had a window, 2 cm wide vertically and 0.5 cm wide horizontally, was rotated horizontally around the fiber end within the plane that contains the fiber axis. The distance between the fiber end and the phototube was 12 cm. The samples we tested were clear fibers connected to Y11 waveshifting fibers where LED light was injected. All the possible combinations of single-clad and multiclad fibers were tested. The junction was left with an air gap.

Fig. 8 shows the emission angle distributions measured at the end of 30 cm long clear fiber connected to a 30 cm long Y11 fiber with a type B connector. The distributions are normalized to the data at $\theta = 0°$. The distribution is wider for the combination of multiclad Y11 and multiclad clear fibers than other combinations. The width of the emission angle distribution (half width at half maximum) is 40° for the multiclad fibers, whereas it is about 35° for the other cases. In the figure, the emission angle distributions for 60 cm long multiclad and single-clad Y11 fibers without a connector are shown by the lines. The half width at half maximum were 46° and 37°, respectively. The connector is losing a fraction of the light that is emitted at larger angles. We have performed a Monte Carlo simulation of the emission angle distribution. The result was that the angle is 42° for multiclad fibers and 36° for single-clad fibers when the reflection between the (outer) clad and the air is set not to be allowed. The data with the connector used are consistent with the simulation data and, therefore, we can conclude that the connector is loosing the light trapped at the outermost surface of the fiber and the effect on the other light trapped at the inner layer(s) is small.

4. Summary

We have developed fiber-to-fiber connectors for plastic optical fibers of 0.83, 0.90 and 1.00 mm in diameter. Two types of 10-fiber connectors showed a light transmission of 85–90% with a uniformity of 2.5–3.1%, and a connector reproducibility of 1%. Durability of the connector is satisfactory for our need; The connector showed stable transmission up to the 50 disconnection and re-connections cycles we examined. The transmission was stable to 0.5% after heat cycles. The connectors with these performance results are satisfactory for the CDF endplug upgrade based on a tile/fiber calorimeter technique. Although use of optical matching grease at the joints can further improve the light transmission and uniformity, the transmission with grease was found to be unstable after the heat cycles. Possible use of soft silicone rubber based index matching film is under study.

In order to evaluate the effect of the connector on the light transmission mechanism, we measured the light emission angle distributions for all the possible connection combinations of multiclad and single-clad fibers. Although light emitted at larger angles was found to be partially lost, the connection of multiclad to multiclad fibers showed substantially wider angle distribution than any other combinations.

References

[1] G. Apollinari, P. de Barbaro and M. Mishina, CDF end plug calorimeter upgrade project, Proc. 4th Int. Conf. on the Calorimetry in the High Energy Physics, La Biodola, Elba, September 19–25, 1993.

[2] K. Hara et al., Splicing of plastic fibers using a PEEK tube, Nucl. Instr. and Meth. A 348 (1994) 139.

[3] MCP-10P-1A and MCP-10P-1B are the DDK catalog numbers for Type A for 0.83 mm ϕ and 0.90 mm ϕ fibers, respectively; MCP-10P-2 is that for Type B.

[4] Kuraray single-clad fibers have a polystyrene ($n = 1.59$) core and a PMMA ($n = 1.49$) clad. The multiclad fibers have a fluorinated MMA ($n = 1.42$) in addition as the outer cladding.